

## Micromechanisms of Fracture



Gilbert Hénaff - 2016

1

### Outline

- Introduction/ objectives
- Types of fracture in metals
- Fractographic observation in brittle fracture
- Intergranular fracture
- Theoretical cohesive strength of metals
- The development in theories of brittle fracture
- Ductile fracture
- Ductile to brittle transition behaviour
- Factors affecting modes of fracture



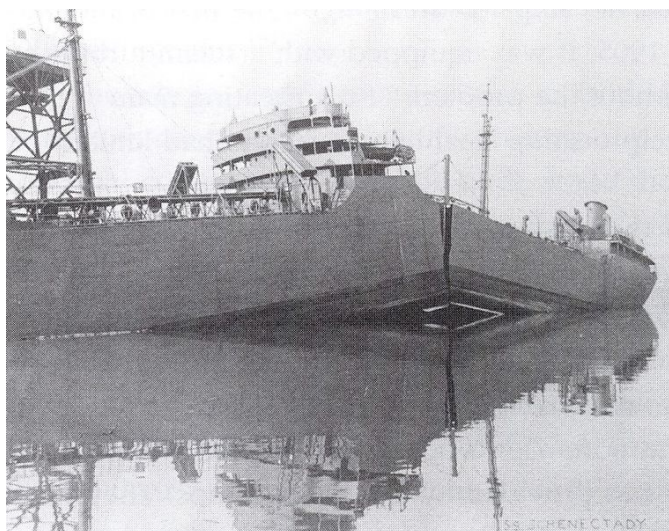
Gilbert Hénaff - 2016

2

## Objectives

- This chapter presents:
  - the theories of brittle and ductile fractures together with the micromechanisms of fracture that might occur in metallic materials.
  - Factors affecting different types of fracture processes such as brittle cleavage fracture, ductile failure or intergranular fracture will be discussed.

## USS Schenectady



## Failure of Liberty Ships



Gilbert Hénaff - 2016

5

## Failure of Liberty Ships

Date: January 16, 1943

Location: Portland Oregon

Temperature: Water 29.2°F : Air 37°F

Construction: Welded

Material: Steel- type unknown

Significant Characteristics: Rapid construction,  
No Crack arresting plates, Inexperienced  
welders Poor construction quality

Point of Origin: Corners of Hatch opening,

Number of ships that failed; 1943 -20 1944-



Gilbert Hénaff - 2016

6

# Failure of Liberty Ships

## Significant contributors to failure:

- Poor quality steel
- New construction methods (welding)-thought to be an unsuitable method of construction
- Lack of knowledge of fracture characteristics of steel,
- Cold, North sea water,
- Overloading.



Gilbert Hénaff - 2016

7

« Famous » failures and associated progresses

Failure	Year	Reason for failure	Life-assessment developments
<i>Titanic</i>	1912	Ship hits iceberg and watertight compartments rupture.	Improvement in steel grades Safety procedures established for lifeboats
Molasses tank failures	1919, 1973	Brittle fracture of the tank as a result of poor ductility and higher loads	Warning systems established for icebergs Design codes for storage tanks developed
Tacoma bridge failure	1940	Aerodynamic instability and failure caused by wind vortices and bridge design	Consideration given to causes for brittle fracture Sophisticated analytical models developed for resonance Bridge design changed to account for aerodynamic conditions
World War II Liberty ships	1942-1952	1289 of the 4694 warships suffered brittle fracture or structure failure at the welded steel joints.	Selection of increased toughness material Improved fabrication practices Development of fracture mechanics
Liquefied natural gas (LNG) storage tank	1944	Failure and explosion of an LNG pressure vessel due to a possible welding defect and improperly heat treated material resulting in subsequent fatigue crack growth	Selection and development of materials with improved toughness at the service temperature of -160 °C (-250 °F)
Comet aircraft failures	1950s	Fatigue crack initiation in pressurized skins due to high gross stresses and stress-concentration effects from geometric features	Development of the fatigue "safe-life" approach Evaluation of the effects of geometry and notches on fatigue behavior Evaluation of the effects of stiffeners on stress distribution
F-111 aircraft No. 94 wing pivot fitting	1969	Fatigue failure due to material defect in high-strength steel	Establishment of aircraft structural integrity program (ASIP) in 1958 Improved inspection techniques Change from fatigue "safe-life" to damage-tolerant design philosophy
Seam-welded high-energy piping failures	1986-2000	Cavitation and creep voids in welds resulting in catastrophic high-energy rupture	Development of materials with improved toughness Development of elevated-temperature life-assessment techniques for cavitation and creep failure
Aloha incident, Boeing 737	1988	Accelerated corrosion and multiple fatigue crack-initiation sites in riveted fuselage skin	Improved aircraft maintenance and inspection procedures Life-assessment methods developed for multiple-site damage (MSD)
Sioux City incident	1989	Hard alpha case present in titanium fan disk resulted in fatigue crack initiation and catastrophic failure.	Increased process controls on processing of titanium ingots Development of probabilistic design approach and analytical life assessment using dedicated computer programs for titanium disks
Earthquake in Kobe City, Japan, and Northridge, California	1994, 1995	Failure occurred in I-beams and columns due to joint configuration and welding practices that resulted in low ductility of the steel.	Development of earthquake-resistant structures Improved joint designs and welding practices for structural steels Improved controls on steel manufacture

Source: Ref 1

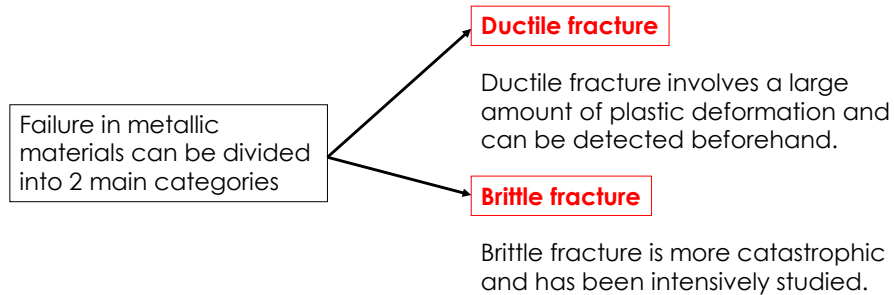


Gilbert Hénaff - 2016

8

## Types of Fracture in Metals

- Materials strength and fracture resistance have been studied for a long time to overcome failures
- The introduction of « malleable » irons during the evolution of material construction led to the perception of brittle and ductile fractures



## Brittle Fracture

## Introduction

- fcc metals: cross slip  $\Rightarrow$  (more or less) ductile fracture at any temperature
- cc and hc metals: cleavage fracture at low temperatures (limited number of slip systems)
- Intergranular fracture: presence of segregated species along grain boundaries

## Cleavage (1)

- Cleavage fracture along  $\{100\}$  planes in cc,  $\{0001\}$  planes in hc
- Propagation perpendicular to the direction of the maximum principal stress

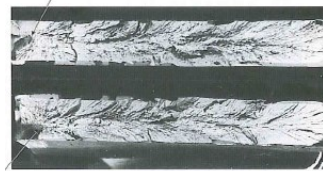
## Fractographic observation of brittle fracture by cleavage

The process of cleavage fracture consists of three steps:

- 1) Plastic deformation to produce dislocation pile-ups.
- 2) Crack initiation.
- 3) Crack propagation to failure.

Distinct characteristics of brittle:

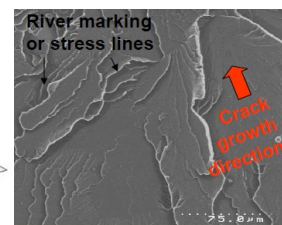
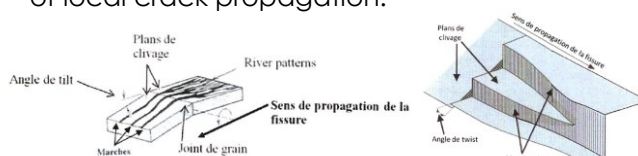
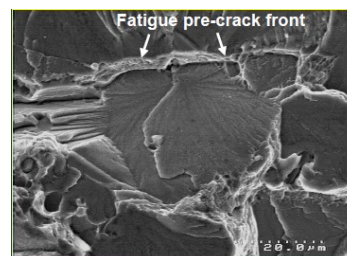
- 1) The absence of gross plastic deformation.
- 2) Grainy or faceted texture.
- 3) River marking or stress lines.



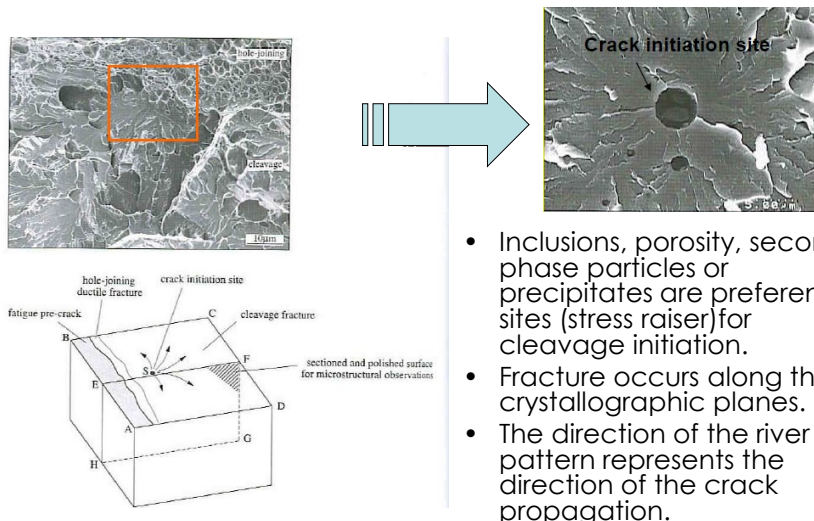
Brittle fracture indicating the origin of the crack and crack propagation path

## Cleavage fracture surface

- Cleavage fracture surface is characterised by flat facets (with a size similar to the grain size).
- The most favorable cleavage plane in an adjacent grain differs by a tilt or a twist angle.
- River lines or the stress lines are steps between cleavage on parallel planes and always converge in the direction of local crack propagation.

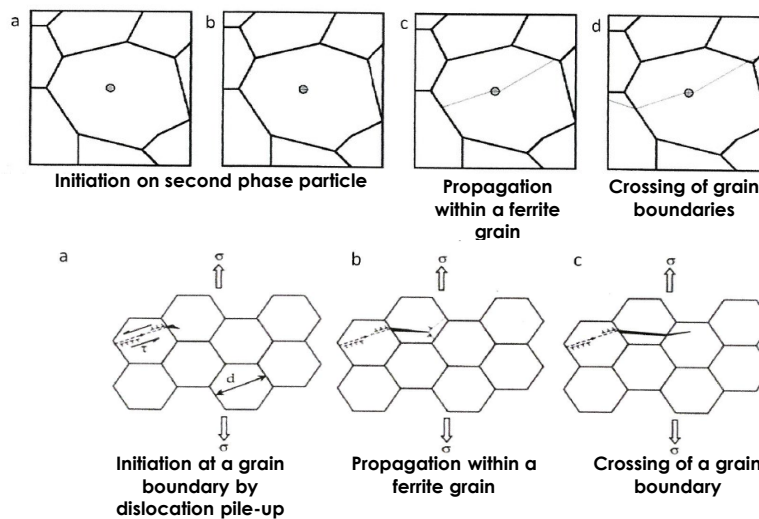


## Crack initiation from particles in cleavage fracture



- Inclusions, porosity, second phase particles or precipitates are preferential sites (stress raiser) for cleavage initiation.
- Fracture occurs along the crystallographic planes.
- The direction of the river pattern represents the direction of the crack propagation.

## Microstructural barriers



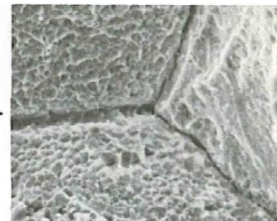
Depending on microstructure, cleavage can be controlled by nucleation of crack embryo or by the crossing of grain boundaries and subsequent propagation.



## Intergranular fracture

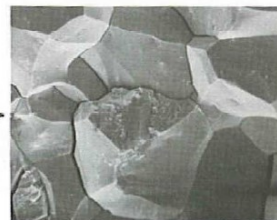
- Intergranular failure is a moderate to low energy brittle fracture mode resulting from grain boundary separation or segregation of embrittling particles or precipitates.

Intergranular fracture with microvoid coalescence

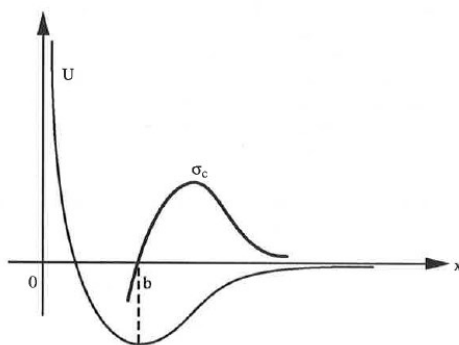


- Embrittling grain boundary particles are weakly bonded with the matrix, high free energy and unstable, which leads to preferential crack propagation path.

Intergranular fracture without microvoid coalescence



## Theoretical cohesive strength of metals



$$\sigma_{\max} = \left( \frac{E\gamma_s}{a_0} \right)^{1/2}$$

The load to move the cleavage apart is determined by the derivative of the cohesion energy with respect to the displacement. Besides cleavage requires an energy corresponding to the creation of 2 new surfaces  $2\gamma_s$ . This relation provides values of the fracture strength that are several orders of magnitude higher than the values experimentally measured.

## Theories of brittle fracture

- Griffith theory of brittle fracture
  - The first analysis on cleavage fracture was initiated by Griffith using the concept of energy balance in order to explain discrepancy between the theoretical cohesive strength and observed fracture strength of ideally brittle material (cf. *Fracture Mechanics course*).
- The development in cleavage fracture models
  - Modified Griffith theory by Irwin and Orowan.
  - Zener's model of microcrack formation at a pile-up of edge dislocations.
  - Stroh's model of cleavage crack formation by dislocation pile-up.
  - Cottrell's model of cleavage crack initiation in BCC metals
  - Smith's model of microcrack formation in grain boundary carbide film.



Griffith (1920) The Phenomena of Rupture and Flow in Solids, *Philosophical Transactions of the Royal Society, A*, 221, 163-198

## Griffith Theory of Brittle Fracture

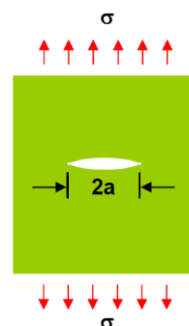
- Observed fracture strength is always lower than theoretical cohesive strength: Griffith explained that the discrepancy is due to the inherent defects in brittle materials leading to stress concentration → lower the fracture strength of the materials.
- Crack propagation criterion: crack growth occurs when the released elastic strain energy is at least equal to the energy required to generate new crack surface

$$\sigma_c = \left( \frac{2E\gamma_s}{\pi a} \right)^{\frac{1}{2}}$$

Plane stress

$$\sigma_c = \left( \frac{2E\gamma_s}{(1-\nu)^2 \pi a} \right)^{\frac{1}{2}}$$

Plane strain



## Modified Griffith Equation

- The Griffith equation is strongly dependent on the crack size  $a$ , and theoretically satisfies only ideally brittle materials like glass.
- However, metals are not ideally brittle and normally fail with certain amounts of plastic deformation, the fracture stress is increased due to blunting of the crack tip.
- Irwin and Orowan suggested Griffith's equation can be applied to materials that can withstand plastic deformation before brittle failure by including the plastic work,  $\gamma_p$ , into the total elastic surface energy required to extend the crack wall, giving the modified Griffith's equation as follows:

$$\sigma_c = \left( \frac{2E(\gamma_p + \gamma_s)}{(1-\nu)^2 \pi a} \right)^{\frac{1}{2}} \approx \left( \frac{E\gamma_p}{(1-\nu)^2 a} \right)^{\frac{1}{2}}$$



Gilbert Hénaff - 2014

21

## Curry's and Knott model for crossing microstructural barriers

- Initiation takes place on second phase particle; crack then propagates until it is arrested at a microstructural barrier (Ex: propagation through bainitic laths and arrest on a grain boundary)
- Unstable crack propagation is determined in the framework of brittle fracture mechanics: the crossing of the barrier occurs as soon as the most critical crack satisfies the Griffith criterion:

$$\sigma_c = \sqrt{\alpha \frac{E\gamma_m}{\pi a_c}}$$

$\alpha$ : coefficient dependent on the shape of the microcrack;

$E$ : Young's modulus;

$\gamma_m$ : effective surface energy accounting for the plastic work dissipated during microcrack propagation;

$a_c$ : critical length of a crack initiated



Gilbert Hénaff - 2016

22

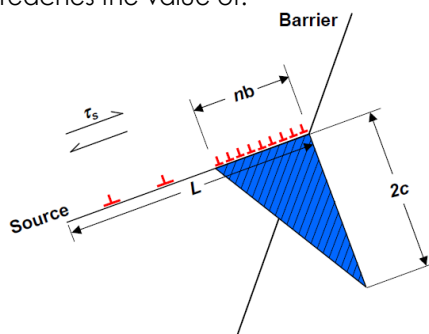
## Zener's model of microcrack formation at a pile-up of edge dislocations

The Griffith theory only indicates the stress required for crack propagation of an existing crack of length  $2a$ , but does not explain the nucleation of the crack.

Zener and Stroh showed that the crack nucleation of length  $2c$  occurs when the shear stress  $\tau_s$  created by pile-up of  $n$  dislocations of Burgers vector  $b$  at a grain boundary reaches the value of:

$$\tau_s \approx \tau_i + \left( \frac{2\gamma_s}{nb} \right)$$

Where  $\tau_i$  is the lattice friction stress in the slip plane.



Gilbert Hénaff - 2016

23

## Stroh's model of cleavage crack formation by dislocation pile-up

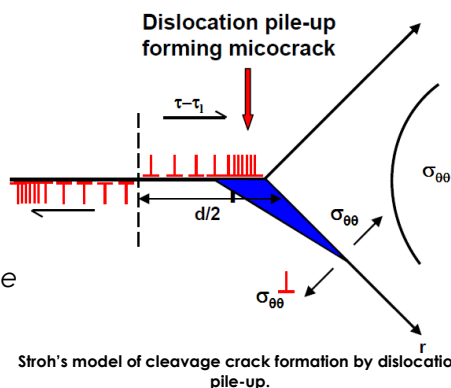
Stroh included the effect of the grain size  $d$  in a model, suggesting the condition of the shear stress created by dislocation pile-up of length  $d/2$  to nucleate a microcrack as follows:

$$\tau_{\text{eff}} \approx \tau_y - \tau_i \sqrt{\frac{E\pi\gamma}{4(1-\nu^2)d}}$$

Where:

- $\tau_{\text{eff}}$  is the effective shear stress
- $\tau_y$  is the yield stress

*Note: This model indicates that the fracture of the material should depend only on the shear stress acting on the slip band.*



Gilbert Hénaff - 2016

24

## Cottrell's model of cleavage crack initiation in bcc metals



Sir Alan Cottrell (1919-2012)

- Cottrell later suggested that the fracture process should be controlled by the critical crack growth stage under the applied tensile stress, which requires a higher stress than the crack nucleation itself as suggested by Stroh.
- Cottrell also showed that the crack nucleation stress can be small if the microcrack is initiated by intersecting of two low energy slip planes to provide a preferable cleavage plane.

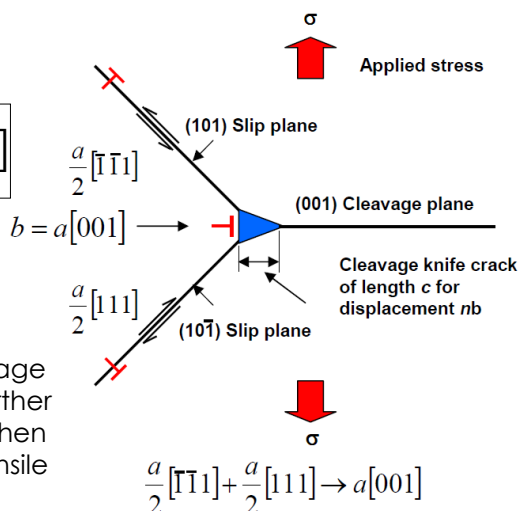


Gilbert Hénaff - 2016

25

## Cottrell's model of cleavage crack initiation in bcc metals

$$\frac{a}{2}[\bar{1}\bar{1}1] + \frac{a}{2}[111] \rightarrow a[001]$$



This results in a wedge cleavage crack on the (001) plane. Further propagation of this crack is then controlled by the applied tensile stress.

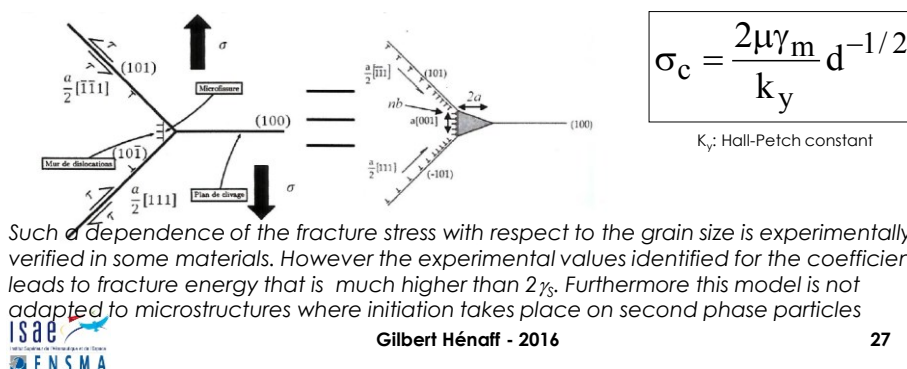


Gilbert Hénaff - 2016

26

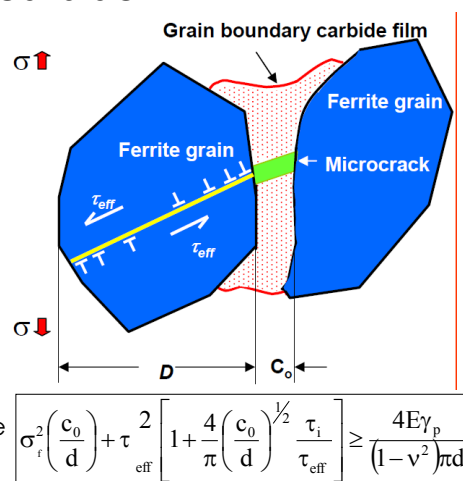
## Cottrell's model of cleavage crack initiation in bcc metals

- The dislocation created to minimize the energy is equivalent to a wedge of height  $nx$  ( $n$ : number of dislocations,  $b$ : Burgers vector) and length  $2a$ ;
- Cottrell calculates the critical energy required to create this sessile « superdislocation »
- Instability analysis → critical cleavage stress  $\sigma_c$



## Smith's model of microcrack formation in grain boundary carbide film

- Models proposed by Stroh and Cottrell involve crack initiation by dislocation pile-up of length  $D/2$ , but do not consider the role of second phase particles (cementite in mild steels for instance).
- Smith then proposed a model for cleavage fracture in mild steel related to microcracking of grain boundary carbide by dislocation pile-up of length equal to half of the grain diameter  $d/2$ .
- Microcrack is initiated when a sufficiently high applied stress causes local plastic strain within the ferrite grains to nucleate microcrack in brittle grain boundary carbide of thickness  $C_0$ .



Note: Further propagation of the GB carbide crack follows the Griffith theory.

## Smith's model of microcrack formation in grain boundary carbide film

- When the term related to dislocation pile-up is neglected, the criterion for propagation based on critical stress is similar to Griffith criterion

$$\sigma_f^2 \left( \frac{c_0}{d} \right) + \tau_{\text{eff}}^2 \left[ 1 + \frac{4}{\pi} \left( \frac{c_0}{d} \right)^{1/2} \frac{\tau_i}{\tau_{\text{eff}}} \right] \geq \frac{4E\gamma_p}{(1-\nu^2)\pi d}$$

## Smith's model of microcrack formation in grain boundary carbide film

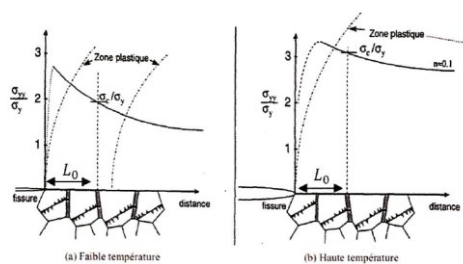
- At the flow stress, using the Hall-Petch relation, it appears that the ferrite grain does no longer intervene in the formula while experimental data indicate that the cleavage strength in mild steels depends on  $d^{1/2}$ .

$$\sigma_f^2 c_0 + \left[ 1 + \frac{4}{\pi} (c_0)^{1/2} \frac{\tau_i}{k_y} \right] \geq \frac{4E\gamma_p}{(1-\nu^2)\pi}$$

- However it has been shown that these parameters are not disconnected; indeed a fine grain size is associated to small carbides.

## RKR model

- The model proposed by Ritchie, Knott and Rice tries to relate the critical stress  $\sigma_c$  to the fracture toughness  $K_{IC}$ .
- In this model, fracture occurs when the maximum principal stress reaches the critical stress value at a distance equal to  $L_0$  from the crack tip.
- $\sigma_c$  and  $L_0$  do not depend on temperature;
- $K_{IC}$  depends on yield stress  $\sigma_y$  and therefore on temperature;
- At low temperatures, lower stresses are required to reach the critical stress value and vice versa;

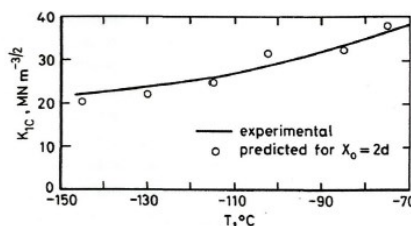


$$K_{IC} = \beta^{-(n+1)/2} L_0^{1/2} \left[ \frac{\sigma_c^{(n+1)/2}}{\sigma_y^{(n-1)/2}} \right]$$

$\beta$ : amplitude of the stress singularity;  
 $n$ : strain hardening coefficient

## RKR model

- $L_0 \sim 2 \times \text{grain size } d$
- $L_0$  and  $\sigma_c$  have to be derived from experimental data;





## Weakest link theory

- In a given material, the stressed region (volume  $V$ ) is divided into  $N$  elements (volume  $V_0$ ).
- Each volume is submitted to a homogeneous stress  $\sigma_i$  and the probability of failure is  $p_0(\sigma_i)$ ;
- The probability of failure of the total volume is:

$$P_r(\sigma) = 1 - \prod_{i=1}^N (1 - p_0(\sigma_i))$$

- If the stress  $\sigma$  and the failure probability  $p_0(\sigma)$  are the same in each elementary volume,

$$P_r(\sigma) = 1 - (1 - p_0(\sigma))^N = 1 - \exp \left[ \frac{-V}{V_0} \ln \left( \frac{1}{1 - p_0(\sigma)} \right) \right]$$

- If the stress is not homogenous over the volume  $V$

$$P_r(\sigma) = 1 - \exp \left[ - \int_V \ln \left( \frac{1}{1 - p_0(\sigma)} \right) \frac{dV}{V_0} \right]$$



Gilbert Hénaff - 2016

33

## Weibull theory

- In Weibull's model the material is assumed isotropic and statistically homogeneous
- Weibull proposed an empirical relationship:

$$\ln \left( \frac{1}{1 - p_0(\sigma)} \right) = \left( \frac{|\sigma - \sigma_0|}{\sigma_u} \right)^m \quad \sigma - \sigma_0 = 0 \quad \text{if} \quad \sigma - \sigma_0 < 0$$

$\sigma_0$  : threshold stress ( $\sigma_0$  below no failure),  $\sigma_u$  normalising stress.

$$P_r(\sigma) = 1 - \exp \left[ - \int_V \left( \frac{|\sigma - \sigma_0|}{\sigma_u} \right)^m \frac{dV}{V_0} \right]$$



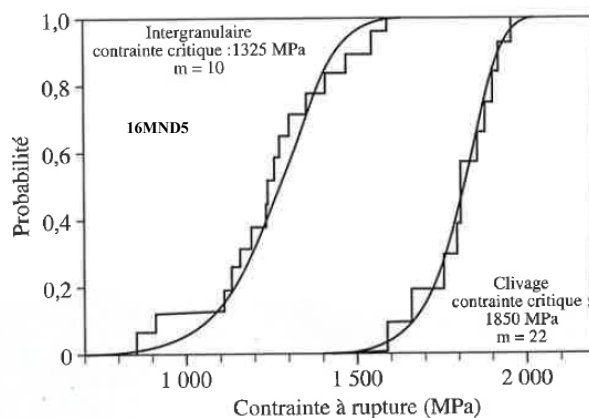
Gilbert Hénaff - 2016

34

## Comments on Weibull's model

- Weibull's model is intrinsically based on probability and macroscopic;
- It recognises the presence of defects and their role as a source of failure, but does not directly consider this presence;
- The model addresses the consequence of the presence of defects but not to the root cause of these defects;
- It does not consider the distribution, orientation, nature of defects and the stress field;
- However this model is simple, with 2 parameters that can be easily experimentally determined on the basis of fracture data;
- It can account for the scatter in fracture data in a wide range of materials (not only in metals!) for simple sollicitations

## Competition between intergranular fracture and cleavage



Intergranular fracture not only occurs at lower stress but the dispersion is also larger, as indicated by the  $m$  value

## Competition between intergranular fracture and cleavage

- Grain boundaries, joining two desoriented lattices, have their cohesion energy  $\gamma_{GB}$  function of the disorientation.
- When failure occurs along a grain boundary, this energy has to be subtracted to the fracture energy  $2\gamma_s$ .
- While the anisotropy of fracture energy has to be taken into account, the cleavage fracture energy is lower than the grain boundary failure energy. One can consider that they are in a ratio of 1.2.
- Intergranular failure will occur if  $R_{CI}$  is lower than 1, where  $R_{CI}$  is defined as:

$$R_{CI} = \left( \frac{2\gamma_{\text{inter}} - \gamma_{GB}}{2\gamma_{sc}} \right) = 1.2 - \frac{\gamma_{GB}}{2\gamma_{sc}}$$



Gilbert Hénaff - 2016

37

## Competition between intergranular fracture and cleavage

- According to Cottrell, the ratio  $\gamma_{GB}/\gamma_{sc}$  is related to the ratio  $\mu/k$  ( $\mu$ : shear modulus;  $k$ : compressibility modulus).

$$R_{CI} = 1.2 - \alpha \frac{\mu}{k}$$

- Detailed calculation in pure Nickel yield:  $\alpha=0.95$ .

	Au	Ag	Cu	Pt	Ni	Rh	Ir	Nb	Ta	V	Fe	Mo	W	Cr
$\mu/k$	0,11	0,19	0,22	0,24	0,34	0,52	0,52	0,25	0,31	0,32	0,33	0,48	0,52	0,82
$R_{CI}$	1,09	1,02	0,99	0,97	0,87	0,71	0,70	0,97	0,91	0,89	0,88	0,75	0,71	0,42



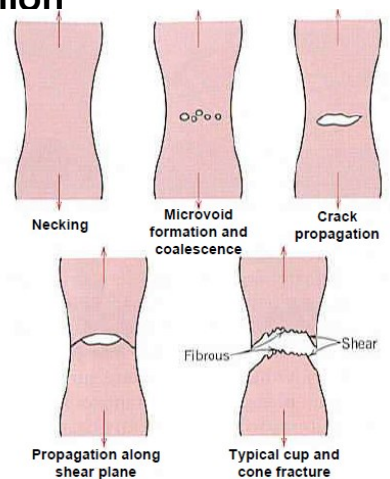
Gilbert Hénaff - 2016

38

## Ductile Failure

### Introduction

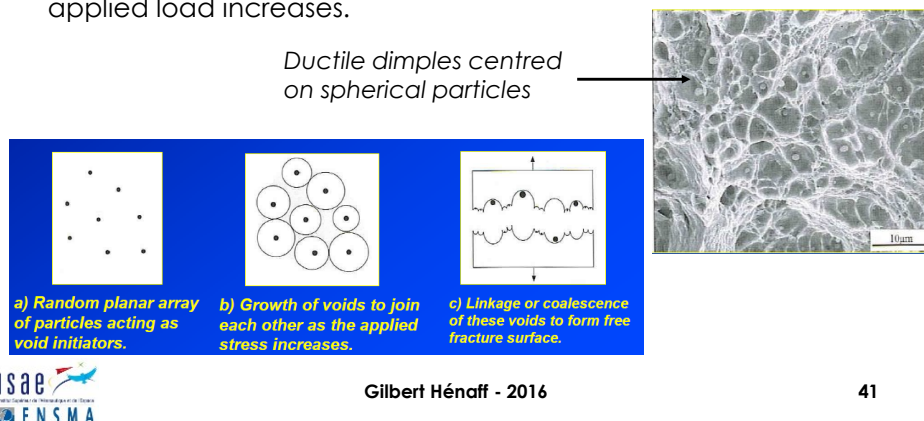
- Ductile fracture is a much less serious problem in engineering materials since failure can be detected beforehand due to observable plastic deformation prior to failure.
- Under uniaxial tensile force, after necking, microvoids form and coalesce to form crack, which then propagate in the direction normal to the tensile axis.
- The crack then rapidly propagate through the periphery along the shear plane at 45°, leaving the cup and cone fracture.



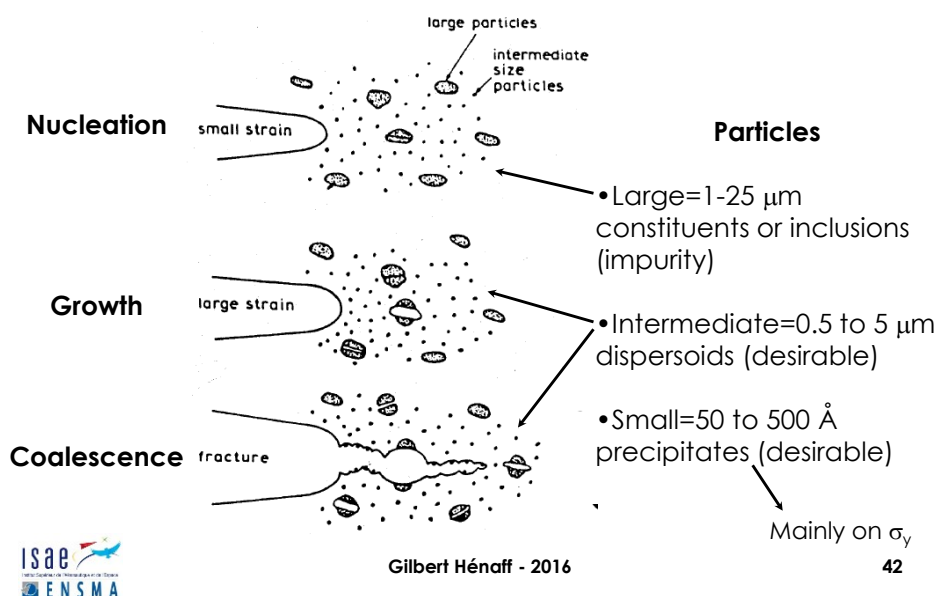
**Definition:** Fracture under continuously increasing stressing, distinguished by purely mechanical nucleation, growth, coalescence of microscopic voids, typically at 2<sup>nd</sup> phase particles

## Microvoid formation, growth and coalescence

- Microvoids are easily formed at inclusions, intermetallic or second-phase particles and grain boundaries.
- Growth and coalescence of microvoids progress as the local applied load increases.

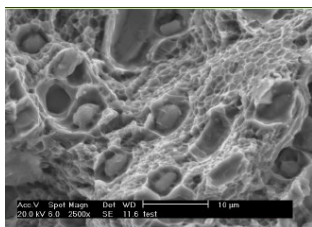


## Stages of dimpled fracture with increased deformation



## Formation of microvoids from second phase particles

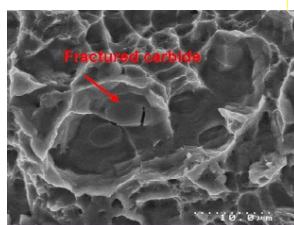
- Microvoids are formed by:
  - 1) Decohesion at particle-matrix interface.
  - 2) Fracture of brittle particle
  - 3) Decohesion of an interface associated with shear deformation or grain boundary sliding.



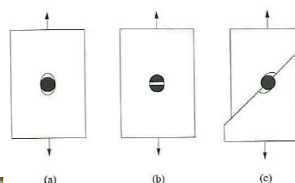
Decohesion of carbide particles from Ti matrix.



Fractured carbides aiding microvoid formation.



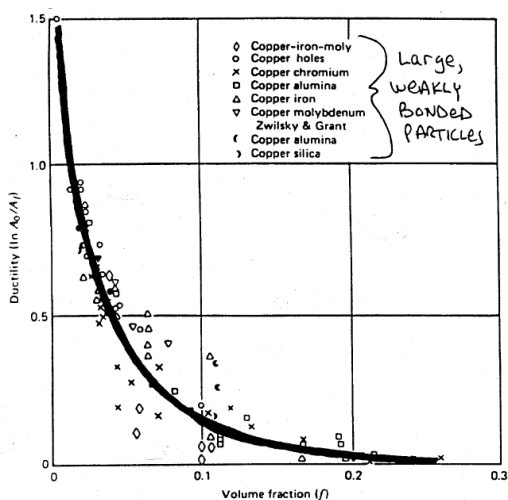
Gilbert Hénaff - 2016



Mechanisms of microvoid formation

43

## Role of 2<sup>nd</sup> phase particles



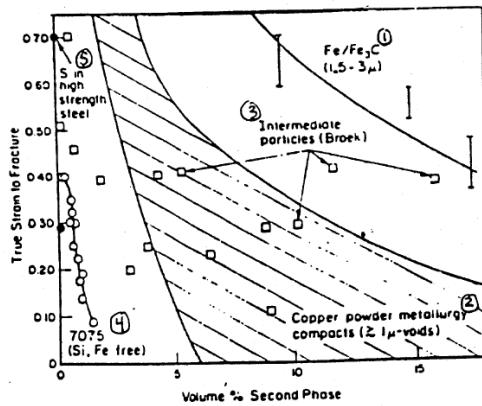
- True fracture stress and strain decrease when the volume fraction of 2<sup>nd</sup> phase particles increases
- The yield strength is not affected by such particles



Gilbert Hénaff - 2016

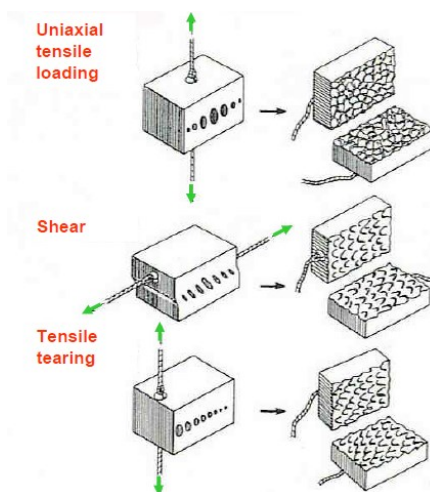
44

## Role of 2<sup>nd</sup> phase particles



1. Carbides in iron
2. Voids in Copper
3. Dispersoids in Al
4. Constituents in 7075
5. Inclusions in steels

## Microvoid shape



Microvoid shape is strongly influenced by the type of loading.

Uniaxial tensile loading → Equiaxed dimples

Shear → Elongated and parabolic dimples pointing in the opposite directions on matching fracture surfaces

Tensile tearing → Elongated dimples pointing in the same direction on matching fracture surface

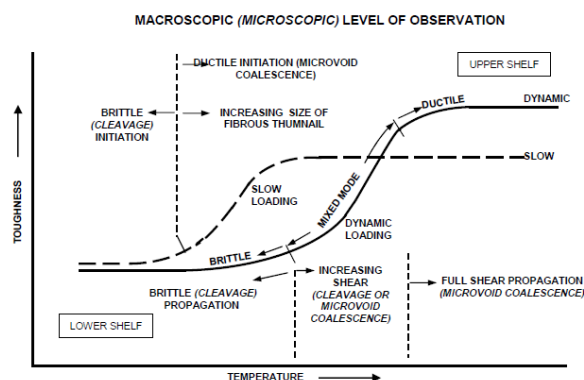
## Ductile fracture resistance

- Depends on:
  - Particle volume fraction
  - Particle size
  - Particle spacing ( $\propto \text{size}/f_v^{1/3}$ )
  - Particle ductility
  - Particle shape
  - Particle-matrix interface strength
  - Matrix work hardening
  - Deformation mode
  - Presence of intermediate size particles

## Ductile to brittle transition

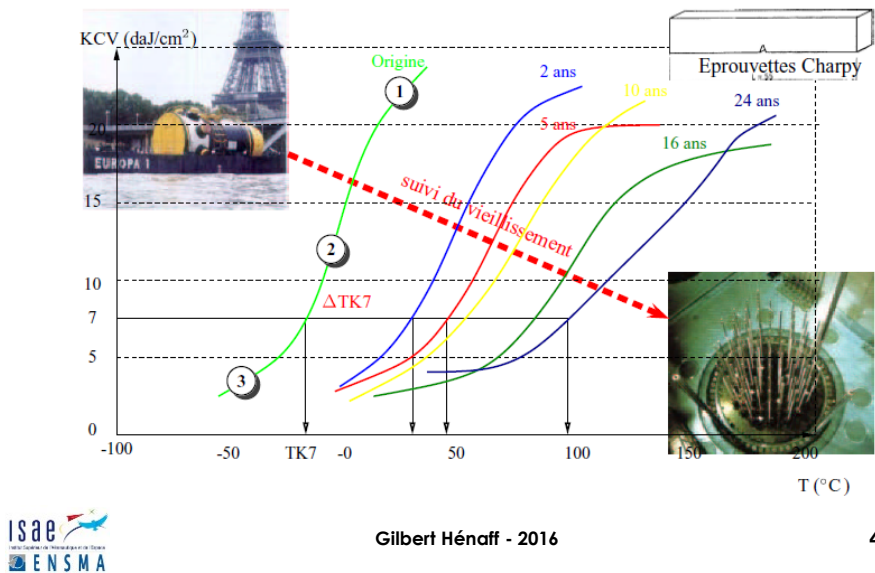
- bcc metals possess limited slip systems available at low temperature, minimising the plastic deformation during the fracture process.
- Increasing temperature allows more slip systems to operate, yielding general plastic deformation to occur prior to failure.

bcc metals experience ductile-to-brittle transition behaviour when subjected to decreasing temperature (and/or high strain rate), resulting from a strong yield stress dependence on temperature.

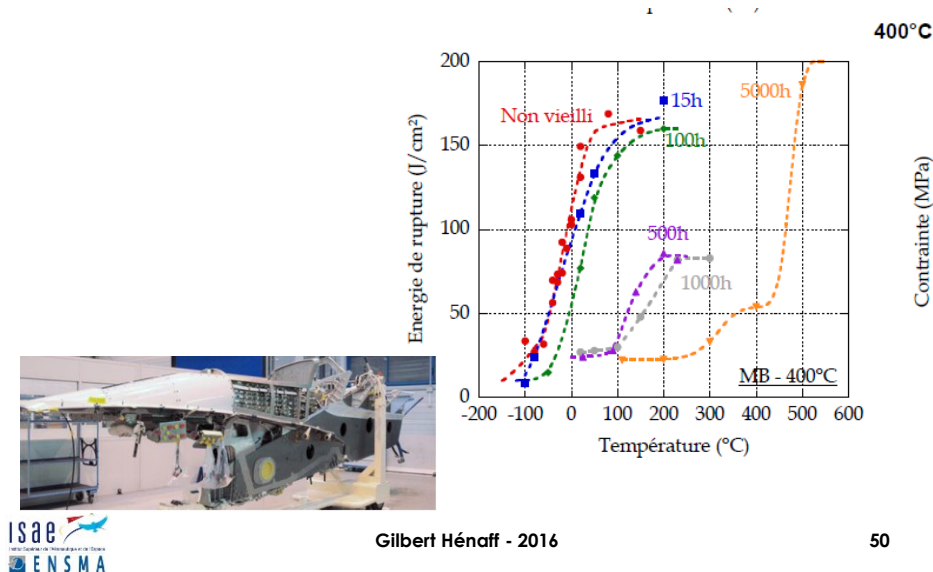




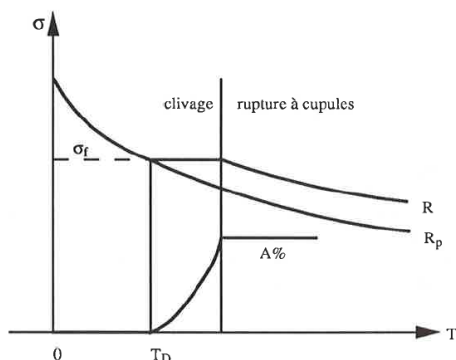
Example: influence of ageing on the DBTT of a nuclear reactor vessel steel



Exemple: influence of ageing on DBTT in a martensitic stainless steel

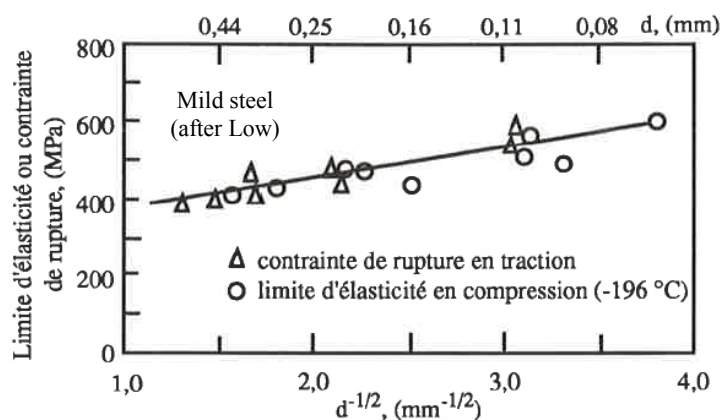


## Ductile to Brittle Transition in smooth specimens



When temperature is lowered, the flow stress increases. Meanwhile, the cleavage critical stress is much less temperature-sensitive. The curves describing their temperature dependence crosses at a temperature  $T_D$ . Just above this temperature, during loading, the material first deforms plastically and work hardening is initiated. Cleavage occurs when the stress reaches  $\sigma_f$ . Elongation at failure thus increases as the difference between  $\sigma_f$  and  $R_p$  is getting larger. Below  $T_D$  failure occurs before reaching the flow stress and elongation at failure is nul.  $T_D$  is the temperature for no ductility on smooth specimens.

## Relation between fracture stress and yield strength at low temperature



## Theory of the ductile to brittle transition

- The criterion for a material to change its fracture behaviour from ductile to brittle mode is when the yield stress at the observed temperature is larger than the stress necessary for the growth of the microcrack indicated in the Griffith theory.
- Cottrell studied the role of parameters, which influence the ductile-to-brittle transition as follows:

$$\left( \tau_i D^{\frac{1}{2}} + k' \right) k' = G \gamma_s \beta$$

*The criterion for ductile to brittle transition is when the term on the left hand side is greater than the right hand*

side

$\tau_i$  is the lattice resistance to dislocation movement;  
 $k'$  is a parameter related to the release of dislocation into a pile-up;  
 $D$  is the grain diameter (associated with slip length);  
 $G$  is the shear modulus;  
 $\beta$  is a constant depending on the stress system.



Gilbert Hénaff - 2016

53

## Factors affecting ductile to brittle transition

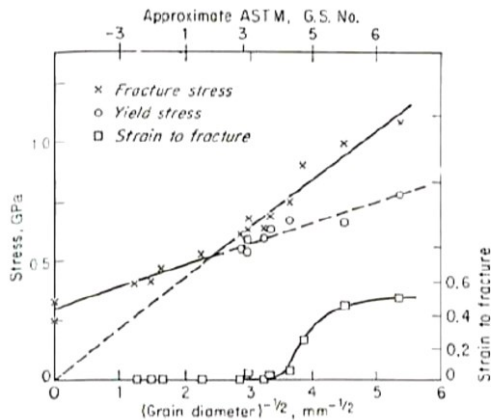
- From equation, materials having high lattice resistance  $\tau_i$ , grain size  $D$  and  $k'$  has a high tendency to become brittle with decreasing temperature.
- The  $\tau_i$  in bcc material is strongly dependent on temperature.
- Materials with high  $k'$  i.e., Fe and Mo are more susceptible for brittle fracture.
- Smaller grain sized metals can withstand brittle behaviour better
- Alloy chemistry and microstructure also affect the ductile-to-brittle transition behaviour.



Gilbert Hénaff - 2016

54

Factors affecting ductile to brittle transition



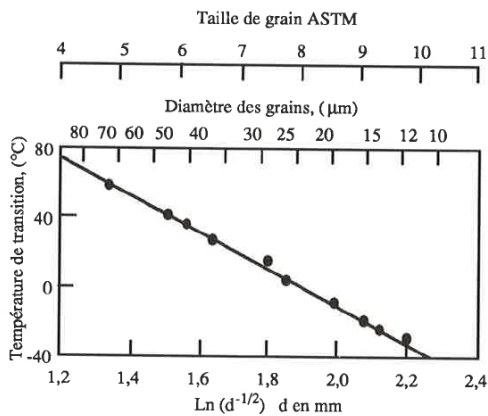
Effect of grain size on the yield and fracture stresses for a low-carbon steel tested in tension at -196°C.



Gilbert Hénaff - 2016

55

Influence of grain size on DBTT



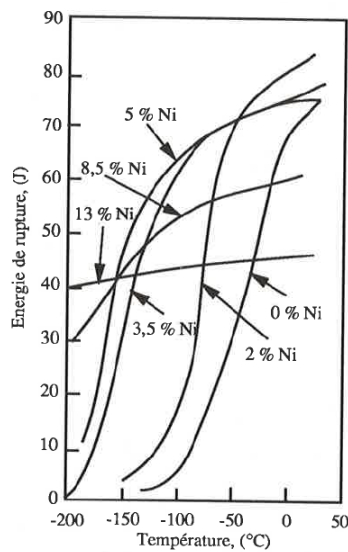
The most important metallurgical parameter is the **grain size**. A smaller grain size induce a higher yield strength according to Hall-Petch law, but also influences the cleavage critical stress. The result is a lower DBTT



Gilbert Hénaff - 2016

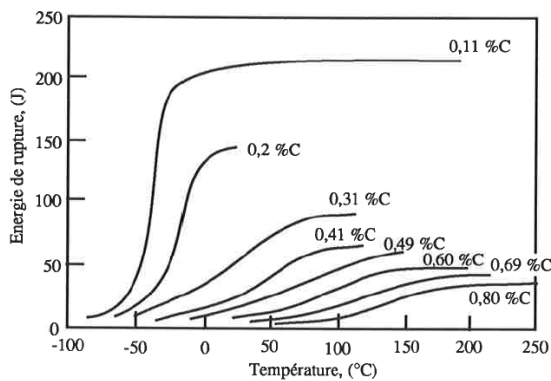
56

## Influence of Ni content on DBTT in steels



Elements such as Ni, by lowering the temperature for austenite transformation, promote the formation of small grains/ therefore they induce a lower DBTT.

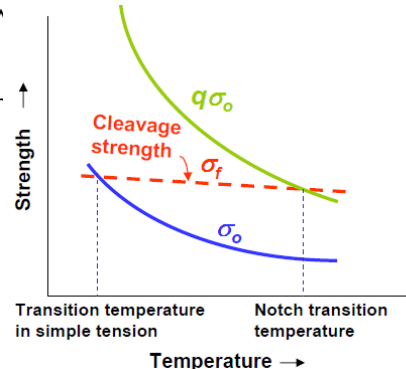
## Influence of interstitials on DBTT



Interstitials such as C or N, by increasing the  $\sigma_0$  term in Hall-Petch relation, make the yield strength to increase and the DBTT. They furthermore affect the ductile plateau.

## Notch effect on transition temperature

- The fracture stress  $\sigma_f$  is much less temperature sensitive than the flow stress  $\sigma_0$ .
- The  $\sigma_0$  of the unnotched specimen is lower than  $\sigma_f$  at temperatures above the transition temperature.
- The metal therefore deforms plastically before fracture. Below the transition temperature  $\sigma_0 > \sigma_f$ , metal fails without plastic deformation.
- The presence of the notch raises the  $\sigma_0$  by the plastic constraint factor  $q$ . This shifts the transition temperature to the right hand side.



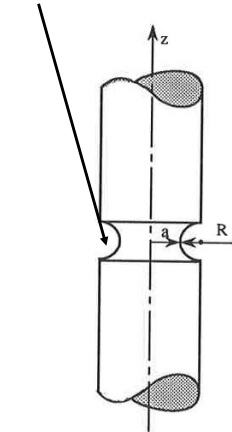
## Influence of stress triaxiality

- In a notch specimen, as far as the gross stress is lower than the yield strength, the maximum of stress is located at the notch root (stress concentration)
- The yield strength is first reached in this site. During further loading, plasticity spreads from the notch root. The load required to spread plasticity across the entire section is generally much larger than the load that would be applied on a smooth specimen of the same section.
- The triaxiality rate can reach very high values

## Notched specimens: Bridgman's analysis

- Hyp: radial and hoop strains are equal and homogeneous in the minimum section  $\Rightarrow \sigma_{rr} = \sigma_{\theta\theta}$

Notch or necking



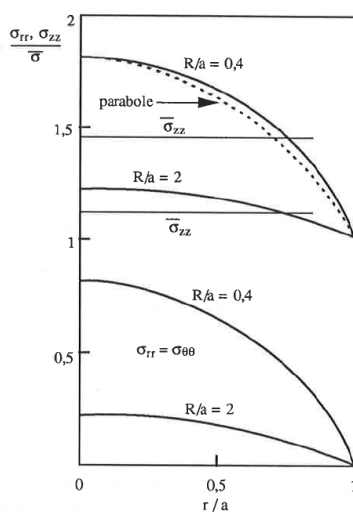
$$\frac{d\sigma_{rr}}{dr} = -\frac{\bar{\sigma}}{\rho} \quad \bar{\sigma} : \text{equivalent stress}$$

$$\rho = \frac{a^2 + 2aR - r^2}{2r}$$

$$\sigma_{rr} = \sigma_{\theta\theta} = \bar{\sigma} \ln \left( 1 + \frac{a^2 - r^2}{2aR} \right)$$

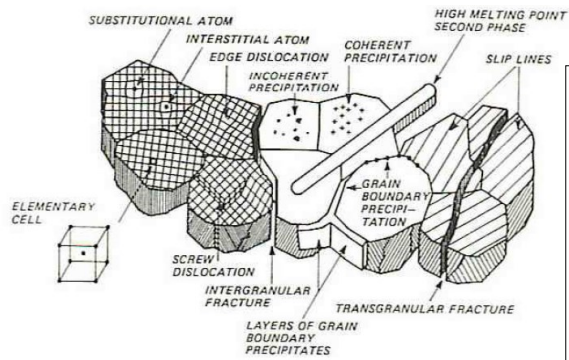
$$\sigma_{zz} = \bar{\sigma} \left[ 1 + \ln \left( 1 + \frac{a^2 - r^2}{2aR} \right) \right]$$

## Notched specimens: Bridgman's analysis



$$\frac{\sigma_m}{\bar{\sigma}} = \frac{1}{3} + \ln \left( 1 + \frac{a}{2R} \right)$$

## Metallurgical aspects of fracture



There are microstructural features that can play a role in determining the fracture path, the most important are:

- Second phase
- Particles and precipitates
- Grain size
- Fibering and texturing

High strength materials usually possess several microstructural features in order to optimise mechanical properties by influencing deformation behaviour / fracture paths.